

REDUCING THE SYNCHROTRON RADIATION ON RF CAVITY SURFACES IN AN ENERGY-RECOVERY LINAC

Georg H. Hoffstaetter*, Matthias Liepe, Tomohiko Tanabe (Cornell University, Ithaca, New York)

Abstract

In Energy Recovery Linac (ERL) light sources, a high energy, high current beam has to be bent into a superconducting linac to be decelerated. The synchrotron radiation produced in the last bending magnet before the linac shines into the superconducting structures if not collimated appropriately. Due to the length of the linac, the radiation cannot be completely guided through the superconducting structure, as in existing SRF storage rings. For the example of an ERL extension to the existing CESR storage ring at Cornell we estimate the magnitude of this problem by quantifying the heat load that can be accepted on a superconducting surface and by analyzing how much radiation is deposited on the cavity surfaces for different collimation schemes.

INTRODUCTION

In the study of an ERL in Cornell's CESR tunnel [1], the superconducting niobium RF cavities are placed a few meters after the bending section [2]. The synchrotron radiation produced by high energy electrons propagates outward, hitting the surface of the RF cavities. This is not desirable since the accumulation of radiation would result in high enough temperature to produce breakdown of superconductivity. Furthermore, it produces photo-emitted electrons which can be accelerated and produce a dark current heat load. In this paper, we investigate the amount of radiation on the RF cavities, and analyze how it can be reduced.

COMPUTATIONAL TOOL

We assume that the particles have Gaussian distributions both in position and velocity in the plane perpendicular to the beam. This we use to compute the four-dimensional synchrotron radiation power distribution, including the $1/\gamma$ angle [2]. Our program slices the dipole magnets into small pieces, each of which projects synchrotron radiation onto a screen. In order to investigate the effect of radiation on cavity walls, the screen was allowed to have an arbitrary angle incident to the beam. Collimators are included by propagating the synchrotron radiation phase space distribution from one collimation plane to the next. The BMAD library [3] was used to propagate the beam.

As a realistic example, Fig. 1 shows the radiation density with the parameters given in Tab. 1.

The cavity was placed 2.5m after the end of the dipole magnet, and the screen was placed perpendicular to the op-

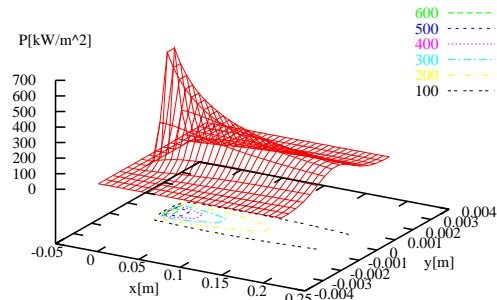


Figure 1: Radiation profile at the cavity entrance.

Parameter	Value
Particle energy [GeV]	3.238
Beam current [A]	.1
Bending radius of dipole magnet [m]	77
Drift distance [m]	2.5
Radius of cavity iris [m]	.035

Table 1: Parameters for the radiation profile.

tical axis at the entrance of the cavity. The radiation density here is too large and must be reduced.

TOLERABLE POWER DENSITIES

Suppose the superconducting cavity is covered in a 2K Helium bath. The niobium surface will then have a higher temperature for two reasons. (a) Energy is deposited in the niobium due to RF fields and the resistivity of the material, and (b) there is a Kapitza conductance that leads to a temperature jump at the surface between the superconductor and helium. The AC surface resistance $R(T)$ of niobium strongly increases with temperature, so that the deposition of synchrotron radiation not only increases the power deposition, but it increases the temperature and thus the power that is absorbed from the RF field. This in turn increases the temperature again, leading to further power absorption.

The radiation power density P_s plus the absorbed RF power $\frac{1}{2}R(T)H^2$ at a magnetic field H constitute the total absorbed power P , which in turn determines the temperature $T(P)$,

$$P_s + \frac{1}{2}R(T(P))H^2 = P. \quad (1)$$

Programs are available to solve this this equation implicitly for P [4], giving the temperature $T(P)$ at the vacuum side of the niobium, and the heat transport equation leads

* Georg.Hoffstaetter@cornell.edu

to the temperature at the helium side of the material. Results are shown in Tab. 2, where a magnetic field at the surface of $H = 840\text{Oe}$ (6.7T) was assumed, corresponding to 20MV/m accelerating field. The last row of this

P_s	$T_{\text{Nb(He)}}$	$T_{\text{Nb(Vac.)}}$	P
1.0kWm^{-2}	2.46K	2.74K	1.43kWm^{-2}
2.0kWm^{-2}	2.58K	2.96K	2.60kWm^{-2}
2.3kWm^{-2}	2.62K	3.02K	3.01kWm^{-2}

Table 2: Temperature of niobium in a helium bath at 2K.

table describes the maximum tolerable radiation power of 2.3kWm^{-2} . Note that this is a conservative estimate of the tolerable synchrotron power, since the areas with largest H are close to the equator and are therefore not irradiated.

Short bunches emit a significant part of their radiation spectrum coherently, leading to strongly enhanced radiation power. For a Gaussian longitudinal bunch profile with bunch length σ_τ this leads to an increase in the total emitted power of approximately [5]

$$\frac{P_{\text{coh}}^{(N)}}{P_{\text{incoh}}^{(N)}} = 0.002237 \frac{\text{GeV}^4}{\text{pC}} \left(\frac{\text{mm}}{\text{m}}\right)^{\frac{4}{3}} \frac{q_{\text{bunch}}}{E^4} \left(\frac{\rho}{\sigma_\tau}\right)^{\frac{4}{3}}. \quad (2)$$

For a bunch length of 0.6mm and a bunch current of 77pC this leads to quite significant coherent synchrotron radiation as shown in Tab. 3 for the bending radii which are used in this study. For the shielding factor of the vacuum pipe we use a formula that was derived for a uniform distribution of length σ_τ ,

$$k_{\text{shield}} = \left(\frac{\sigma_\tau}{\sqrt{3}\rho}\right)^{\frac{1}{3}} \frac{a}{2\sigma_\tau}. \quad (3)$$

For the distance between the shielding vacuum walls parallel to the plane of the orbit we use $a = 2\text{cm}$.

$\rho[\text{m}]$	$\frac{P_{\text{coh}}^{(N)}}{P_{\text{incoh}}^{(N)}}$	k_{shield}	$\frac{P_{\text{tot}}^{(N)}}{P_{\text{incoh}}^{(N)}}$
45	0.50	0.33	1.16
77	1.01	0.28	1.28
393	8.9	0.08	1.71
1291	43.5	0.05	3.34

Table 3: CSR and its suppression for different bending radii.

For the large bending radii the radiation is completely dominated by CSR and an enhancement of 43.5 is possible, which leads to a total power enhancement of only 3.34 due to shielding of CSR by a rather tight vacuum pipe. In the remainder of this report, only the incoherent part of the radiation is computed and plotted since the coherent radiation is in the infrared and has a much larger opening angle than the incoherent radiation. Furthermore, it reflects very well off the niobium walls [6]. For the planned bunch-length of 0.6mm , coherent radiation is enhanced in the region of $\nu = \frac{c}{\sigma_\tau} = 500\text{GHz}$. At these frequencies the reflectivity is

very close to 100% and the coherent radiation is therefore distributed over the total cavity area.

According to [6], photons incident on a superconducting surface can break Cooper pairs and therefore destroy superconductivity. For superconducting niobium the photon-energy threshold for this process is about 750GHz or $\lambda_{\text{cut}} = 0.4\text{mm}$. At this frequency the reflectivity jumps to about 98% and slowly increases with increasing frequency.

ELECTRON EMISSION

The synchrotron radiation can also lead to emission of electrons from the niobium, which in turn can be accelerated and can damage vacuum components. For the parameters in Tab. 1, the characteristic photon energy is $E_c = \hbar\omega_c = \frac{3e\gamma^3}{2\rho} \hbar = 978\text{eV}$. The number of photons per unit time and area is roughly $\frac{d}{da} \dot{N}_{ph} = \frac{15\sqrt{3}}{8} \frac{d}{da} P/E_c$, but not all of these photons have an energy that is larger than the work function of niobium, i.e. 4.3eV .

Table 4 gives the total number of photons per Watt of radiation for the spectrum associated with three different magnet radii. Furthermore it specifies the fraction of these photons with an energy of less than the work function WF . This fraction has been computed by [7],

$$N_{<} = \int_0^{WF} \frac{dn}{dE} dE, \quad \frac{dn}{dE} = \frac{1}{\hbar^2\omega} \frac{dP}{d\omega}, \quad (4)$$

$$\frac{dP}{d\omega} = \frac{1}{\omega_c} S\left(\frac{\omega}{\omega_c}\right), \quad S(x) = x \int_x^\infty K_{\frac{3}{2}}(\xi) d\xi. \quad (5)$$

Assuming a quantum efficiency of 10^{-4} , one can now compute the number of photons emitted per area when it is irradiated by 2kWm^{-2} . Since the synchrotron light arrives at the cavity approximately simultaneously with the electrons that created it, the photo-emitted electrons are accelerated away from the iris when a bunch in the energy recovery phase is passing the iris. Assuming these photons are focused without magnification onto the neighboring iris after gaining 2MeV of energy, the neighboring iris will obtain a sizable heat load due to this electron radiation. This heat load is shown in the last column of Tab. 4.

$\rho(\text{m})$	$N_{ph}(\text{W}^{-1})$	$\frac{N_{<}}{N_{ph}}$	$\frac{dP_e}{da}(\text{kWm}^{-2})$
77	$2.1 \cdot 10^{16}$	20%	1.1
393	$1.4 \cdot 10^{17}$	34%	4.5
1291	$5.8 \cdot 10^{17}$	49%	11.3

Table 4: The electron radiation density due to photo emitted and accelerated electrons.

REDUCING SYNCHROTRON RADIATION

The power density of Fig. 1 is much higher than the 2kWm^{-2} that are tolerable. One may reduce synchrotron radiation by shielding the RF cavities from the radiation with collimators, and by reducing the magnet strength.

The shielding aperture is limited by the beam width, below which the high-energy particles of the order of a few GeV will hit the shielding material, resulting in undesirable scattering. Safety concerns force us to make the window width of the shield much wider than the beam width, ensuring that very few particles will hit the shield.

To reduce the radiation load below 2kWm^{-2} , one could increase the bending radius of the first part of the magnet, so that it becomes shorter and leaves more space for the second magnet with reduced strength.

In the current design, the next to last dipole has a bending radius $\rho = 77\text{ m}$, and the last one has $\rho = 1291\text{ m}$. This scheme produces a radiation density on the cylindrical cavity wall and on the elliptical iris of the TESLA geometry [8] as shown in Fig. 2.

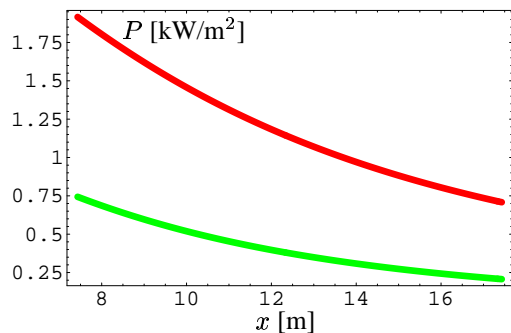


Figure 2: Estimated radiation density on the cylindrical cavity wall with one stronger and one longer magnet and a radiation shield. Computed for the second iris, in the shadow of the first larger iris (green) and for the first iris of a cavity inside a multicell TESLA cavity (red). The first 7.4m can be shielded from synchrotron radiation by collimator in front of the first cryomodule.

While this radiation load seems acceptably small, one should remember that a 6 times larger power from photo-emitted electrons can be expected as listed in Tab. 4.

To further limit the power load, one may reduce the aperture of the higher order mode ferrite dampers to cast a shadow on each cavity, or to put other x-ray collimators inside the linac at appropriate positions. When the ferrite dampers are tilted to cast shadows along the following cavity one has to fear that higher order modes are trapped more easily. However, an analysis of monopole HOMs in the region up to 4GHz shows that such dampers do not change the Q-values of these HOMs as shown in Fig. 3.

CONCLUSION

The power density due to x-rays or photo-electrons hitting a superconducting niobium surface in a 2K helium bath must be limited to 2kWm^{-2} . Achieving this in the suggested ERL in the CESR tunnel will require careful dipole arrangements as well as significant collimation of the synchrotron fan before entering the linac section and within the linac. This first analysis shows that these measures can lead to a reduction of the radiation to about

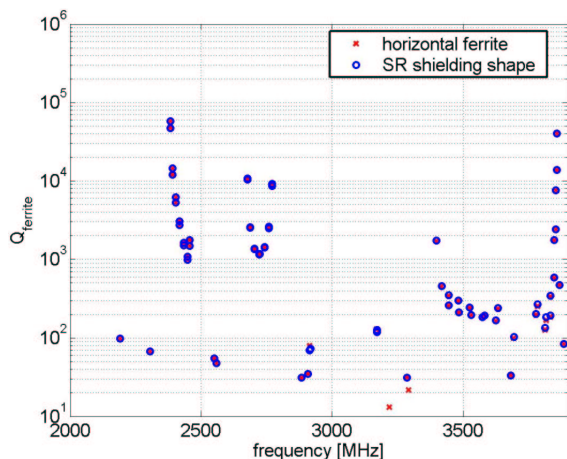


Figure 3: Q-values for the monopole HOMs with standard and tilted ferrite dampers.

700Wm^{-2} for the incoherent radiation. The resulting power due to photon-emitted electrons can however be significantly larger. The power from coherent radiation can be much higher, but can be neglected since it is in the infrared range and is therefore reflected strongly, and is distributed over the complete cavity surface.

Several questions remain: What x-ray and particle radiation are created in the collimation process, and how do they disturb the superconducting cavities? Can reflections of synchrotron radiation that is created upstream of the end of the last magnet be suppressed sufficiently? Can a photo-emitted current be undesirably focused in a way that the high power densities would damage the chamber walls?

REFERENCES

- [1] G. H. Hoffstaetter, I. Bazarov, D. Sagan, R. Talman, Proceedings of PAC'03, Portland (May 2003)
- [2] G. H. Hoffstaetter, T. Tanabe, Reduction of synchrotron radiation of RF cavity surfaces in the proposed Cornell Energy-Recovery Linac, Report Cornell-ERL-04-2 (February 2004)
- [3] BMAD lattice program, maintained by David Sagan, Laboratory of Nuclear Studies, Cornell University (2003)
- [4] Grigori Ereemeev, Cornell University, private communication (2003)
- [5] Phase I Energy Recovery Linac (ERL) Synchrotron Light Source at Cornell University, Report Cornell CHESS-01-003 (2001)
- [6] Terahertz Wakefields in the Superconducting Cavities of the TESLA-FEL Linac, Report DESY (March 2000)
- [7] Matthew Sands, The Physics of Electron Storage Rings, Report SLAC-121 and UC-28 (ACC) (1970)
- [8] TESLA Technical Design Report, Report DESY (1995)